

SEGMENTATION OF DAMAGED BUILDINGS FROM LASER SCANNING DATA

Miriam Rehor and Hans-Peter Bähr

Institute of Photogrammetry and Remote Sensing (IPF), Karlsruhe University, Germany
rehor@ipf.uni-karlsruhe.de, baehr@ipf.uni-karlsruhe.de

Commission III/3

KEY WORDS: LIDAR, Segmentation, Triangulation, Statistics, Classification, Damaged Buildings

ABSTRACT:

Laser scanning- or "LIDAR"-based systems show perfect performance during time-critical events, like data collection in disaster management. To this end the research reports from classification of damaged buildings, a special challenge, for which first results are given. Firstly, mathematical foundations compile some new insights which are specific for the mentioned task, like Bolzano's theorem and statistical tests based on an extended Gauss-Markov model. Secondly, it is presented how these tools support the segmentation of planar surfaces and the classification of TIN segments into undamaged and damaged elements as well as into connecting triangles. Results are presented for real data from a training area of the Swiss Military Disaster Relief. The present status of the investigation shows that clear assumptions can be made for damaged buildings. Further steps will fuse additional knowledge in terms of data and algorithms.

1 INTRODUCTION

Disaster Management issues, unfortunately, are of growing importance worldwide. In any case of disaster, spatial data are the backbone for adequate decisions.

This is particularly true in case of time-critical situations, where the responsible experts have to make their decisions very fast with respect to save as many lives as possible. Therefore, image-based data acquisition including automatic image analysis procedures proves to be an excellent tool in a disaster environment.

More precisely, laser scanning ("LIDAR") shows an ideal performance for such environments due to fast and geometrically precise data. At the IPF the technique has been analysed in the context of strong earthquakes since 1997 (Steinle & Bähr 1999; Vögtle & Steinle 2000). However, a general problem is the lack of "real" laser scanning data from earthquakes or similar occasions: synthetic simulations of destroyed or damaged buildings would never fully reveal what might happen in reality.

This problem has overcome by a laser scanning flight of a camp from the Swiss Military Disaster Relief. The camp contains a complete collection of different types of destroyed or damaged building ensembles. The aim of this publication is to show the performance of laser scanning data for detection and classification of such an environment. This is a challenging new task which starts from the results for modelling undamaged buildings, which have been broadly published (see e.g. Kaartinen et al. 2005; Schwalbe et al. 2005; Steinle 2005).

Before starting, some basic terms have to be clarified. The overall aim is *classification* of damaged buildings recorded by laser scanning in the context of disasters, like earthquakes. Classification means to assign unknown patterns to a priori given classes. The classes are expressed by names (concepts). This is a very important observation, since concepts are by nature ambiguous (Bähr & Müller 2004; Bähr 2005).

The patterns to be classified are the result of a *segmentation* process of the LIDAR point clouds. Therefore, segmentation is a necessary step with respect to the following classification and means division of the point cloud into homogenous features. *Homogeneity* may be very diverse, like patches of similar colour,

shape or orientation, like edges of similar length, width and mutual position and even like point clusters of given distribution. The features extracted in the segmentation process are, nota bene, without any semantics.

Finally, the term *model* needs some comments, since its use is often vague and not clearly defined. In the context of this work the model contains the knowledge (i.e. facts and rules) necessary for segmentation of the point cloud. Subsequently, *modelling* means formalising the physical world in order to make the data fit for reasoning.

2 SOME MATHEMATICAL FOUNDATIONS

2.1 Theory of Model Error Detection in Gauss-Markov Models

In order to check a Gauss-Markov model for model errors, the initial model given by

$$l + v = A \hat{x} \quad \text{and} \quad C_{ll} = \sigma_0^2 Q_{ll} = \sigma_0^2 P^{-1} \quad (1)$$

may be extended. To do this, p new unknowns y are introduced, which compensate gross errors from single observations or from groups of observations (see Baarda 1967; Baarda 1968; Heck 1985; Niemeier 2002).

While the stochastic model remains unchanged, the extended functional model is given by

$$l + \bar{v} = A \hat{x} + B \hat{y}. \quad (2)$$

The matrix B describes the influence of the new parameters y on the observations. Since the residuals and the estimates of the unknowns change in relation to the initial model, these values are written as \bar{v} and \hat{x} . The estimates of the new unknowns are collected in the vector \hat{y} . The extension $B \hat{y}$ may be regarded as an improvement of the initial model. The redundancy \bar{r} of the extended model is given by

$$\bar{r} = \dim(l) - (\dim(\hat{x}) + \dim(\hat{y})) = r - p \quad (3)$$

where r is the redundancy of the initial model.

If B is column-regular, the weighted square sum of the residuals $\bar{\Omega} = \bar{v}^T P \bar{v}$ of the extended model follows from the weighted square sum of the residuals $\Omega = v^T P v$ of the initial model:

$$\bar{\Omega} = \Omega - \hat{y}^T Q_{yy}^{-1} \hat{y} = \Omega - \Delta\Omega \quad (4)$$

with

$$\hat{y} = -Q_{yy} B^T P v \quad \text{and} \quad Q_{yy} = (B^T P Q_{vv} P B)^{-1}$$

This equation shows clearly that the model extension leads to a reduction of the weighted sum of the squares of the residuals. The extension makes sense only if the square sum $\bar{\Omega}$ of the extended model becomes significantly smaller than the respective value from the initial model (Ω). This is precisely the case if $\Delta\Omega$ is significantly larger than zero.

This case may be checked by means of a parameter test. The belief that the model errors are not significant (i.e. the initial model does fit to the physical reality) corresponds to the null hypothesis H_0 . The alternative hypothesis H_A , on the other hand, assumes that model errors do exist and therefore the extended model has to be accepted. In order to test whether the model errors are significant, the weighted square sum $\Delta\Omega$ may be compared to the a priori variance σ_0^2 or to the a posteriori variance $\hat{\sigma}^2$ of the extended model (Niemeier 2002).

The corresponding test statistics are

$$T_1 = \frac{\hat{y}^T Q_{yy}^{-1} \hat{y}}{\sigma_0^2} \sim \chi_{(p,\lambda)}^2 = p \cdot F_{(p,\infty,\lambda)} \quad (5)$$

and

$$T_2 = \frac{\hat{y}^T Q_{yy}^{-1} \hat{y}}{\hat{\sigma}^2} \sim p \cdot F_{(p,r-p,\lambda)} \quad (6)$$

respectively. If $y = E(\hat{y})$ is the expectation of \hat{y} ,

$$\lambda = \frac{y^T Q_{yy}^{-1} y}{\sigma_0^2} \quad (7)$$

is the non-centrality parameter of the (non-central) Fisher distribution and vanishes if H_0 is valid.

2.2 Segmentation of Planar Surfaces

The selected approach for modelling buildings is based on the assumption that undamaged buildings may be represented by planar surfaces. For the extraction of planar surface elements a region growing algorithm is used, taking 2.5D raster data. The starting point for any surface segment is a seed region which fulfils the condition that the n assigned points are approximately located in a plane. The parameters of this plane are determined by least squares adjustment. Owing to only 3 unknowns ($\hat{a}_0, \hat{a}_1, \hat{a}_2$), the solution of the adjustment may be given straightforward by the well known expressions (x_i, y_i : position coordinates; $g(x_i, y_i)$: height):

$$g(x_i, y_i) + v_i = \hat{a}_0 + x_i \hat{a}_1 + y_i \hat{a}_2 \quad (8)$$

$$\begin{pmatrix} \hat{a}_0 \\ \hat{a}_1 \\ \hat{a}_2 \end{pmatrix} = \begin{pmatrix} n & \sum_{i=1}^n x_i & \sum_{i=1}^n y_i \\ \sum_{i=1}^n x_i & \sum_{i=1}^n x_i^2 & \sum_{i=1}^n x_i y_i \\ \sum_{i=1}^n y_i & \sum_{i=1}^n x_i y_i & \sum_{i=1}^n y_i^2 \end{pmatrix}^{-1} \cdot \begin{pmatrix} \sum_{i=1}^n g(x_i, y_i) \\ \sum_{i=1}^n g(x_i, y_i) x_i \\ \sum_{i=1}^n g(x_i, y_i) y_i \end{pmatrix} \quad (9)$$

After determination of the seed region any of the adjacent pixels which were not yet assigned to a surface segment is tested whether it fulfils the planar equation under concern. To this end, in a first step the plane is computed again, based on the enlarged set of points. In a second step it is decided by a global test, involving

$$T_{glob} = \frac{v^T P v}{\sigma_0^2} \sim \chi_r^2, \quad (10)$$

if the null hypothesis can be accepted. v is the column vector of least squares residuals resulting from the enlarged set of points.

Moreover, the model error detection method described in chapter 2.1 is taken in order to check whether the tested point might show a gross error.

In case of rejection of the null hypothesis by either the global test or the model error detection method, the model contains an unacceptable error. As the model was ok before adding the point, the conclusion is that this point does not fit to the plane. The results of the segmentation procedure are stored in a so-called *label image* from where they are taken for further processing.

2.3 Bolzano's Theorem for Retrieving Vertical Planes

By the segmentation of planar surfaces vertical planes cannot be extracted. Therefore, the neighbourhood between the planes may only be determined, for a first step, in relation to the projection of the segments onto the ground plane. By this procedure it is impossible to recognise if adjacent planes do really intersect at their border lines. Due to this situation for any contour line recovered from the ground plane it is necessary to test if a vertical break exists between the two neighbouring segments. In case of detection of such a vertical break, a vertical plane has to be inserted in the course of the border line in order to form a consistent building model.

Based on this procedure it is tested if adjacent planes do really intersect in the vicinity of a common border line. Because of linear height change along the border line it is sufficient to test in the endpoints if there is a significant height difference between the two planes.

The methodology is based on Bolzano's theorem (see Bronstein et al. 2001 (p.61)):

If a function $f(x)$ is defined and continuous on a closed interval $[a, b]$ and the values of the function in the endpoints of the interval $f(a)$ and $f(b)$ have different signs, then there exists at least one value c , where $f(x)$ is zero:

$$f(c) = 0 \quad \text{for} \quad a < c < b.$$

Geometrically spoken, the curve of a continuous function intersects the x -axis at least one time at the transition from one side of the x -axis to the other.

This mathematical theorem is graphically explained and subsumed to the case of segmentation of planes in Figure 1. For any border line of the two planes A and B exist exactly two vertical planes, which respectively contain one of the two endpoints P_A and P_E of the border line and which are orthogonal to that line. By intersecting the two vertical planes with the planes A and B , the four straight lines g_{A_A} , g_{B_A} , g_{A_E} and g_{B_E} are created. More precisely, the lines g_{A_A} and g_{B_A} result from the intersection with the vertical plane which contains P_A , whereas the lines g_{A_E} and g_{B_E} result from the intersection with the vertical plane which contains P_E .

This height checking test investigates whether the straight lines which result from intersection with one of the vertical planes do intersect within a given interval. The value k that defines the interval may be chosen arbitrarily, but it controls the velocity of the procedure and the quality of the final results.

As a straight line is a continuous function, the distance between two straight lines again is continuous. Therefore, instead of testing intersection of two lines within a particular interval, it may be asked whether the function which results from the distance between the two lines shows a zero point within this interval.

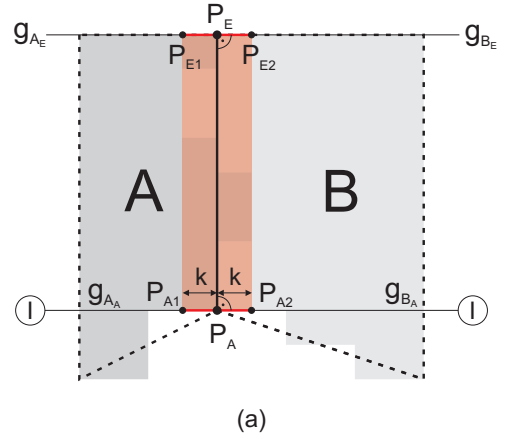
In order to determine if the lines g_{A_A} and g_{B_A} do meet in the interval which is given by P_{A1} and P_{A2} it has to be tested after Bolzano's theorem if the differences d_{A1} and d_{A2} from the functions of both lines show the same sign. If so, the two lines do not meet within the given interval and vice versa (see Figure 1 (b) and (c)).

If both the lines g_{A_A} , g_{B_A} and g_{A_E} , g_{B_E} do intersect within the intervals defined by the points P_{A1} , P_{A2} and P_{E1} , P_{E2} , respectively, the trace of the resulting line in the ground plane is within the red domain of Figure 1 (a). This means that it nearly matches the estimated border line. Consequently, the intersection of this line with other edges will lead to points in the estimated locations. Therefore, in such cases no vertical plane has to be inserted. However, if only one of the two line pairs intersects in the given interval or if no intersection can be determined at all, the vertical gap between the segments A and B in the vicinity of the border line is too large and the intersection is rejected. To make the model consistent, a vertical plane has to be introduced. The equation of this plane may easily be determined by the coordinates of the points P_A and P_E together with the vertical condition.

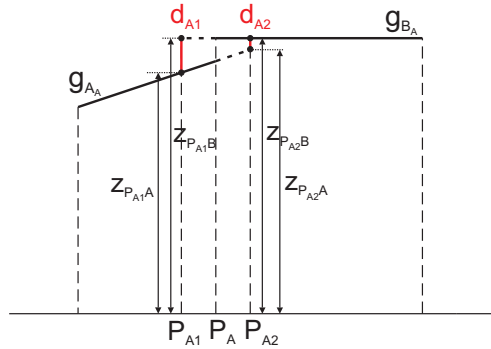
3 FROM SEGMENTS TO CAD MODELS FOR UNDAMAGED BUILDINGS

In order to do the step from single segments to CAD models after completion of the surface segmentation, an analysis of the neighbourhood conditions of the surfaces has to be performed. For this reason by means of morphological operators and starting from the *label image* (see par. 2.2), it is checked in a 2D space which surface segments are adjacent (according to (Steinle 2005)). In a next step the border lines between neighbouring segments are determined. For the itinerary of the border lines it is tested if breaks between adjacent segments do occur, a case which would demand the insertion of a vertical plane. For this procedure the described approach based on Bolzano's theorem is taken (see par. 2.3).

After the topological relations between the single surfaces are known, the lines which describe the edges of the buildings may be determined from intersections of the planes. The topology of the edges is derived indirectly from the neighbourhood conditions of the surfaces, since the edges are not determined directly from



profile ①-①

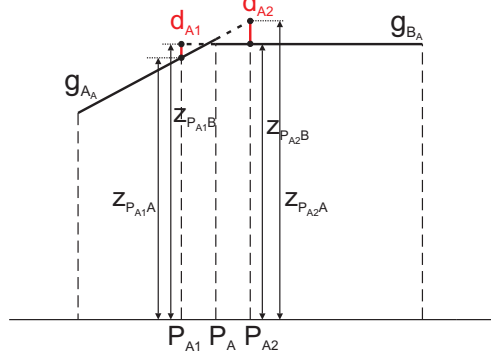


$$d_{A1} = z_{P_{A1}B} - z_{P_{A1}A} > 0$$

$$d_{A2} = z_{P_{A2}B} - z_{P_{A2}A} > 0$$

(b)

profile ①-①



$$d_{A1} = z_{P_{A1}B} - z_{P_{A1}A} > 0$$

$$d_{A2} = z_{P_{A2}B} - z_{P_{A2}A} < 0$$

(c)

Figure 1: Height checking based on Bolzano's theorem; (a) Ground plane; (b) Intersection along profile I - I in case that the straight lines g_{A_A} and g_{B_A} do not intersect in the given interval; (c) Intersection along profile I - I in case that the straight lines g_{A_A} and g_{B_A} do intersect in the given interval

the original data but from plane intersections. The corner points of the buildings are the result of intersecting edges.

Since the geometrical primitives and the corresponding topology is known, it is possible to construct a wireframe model automatically. Commercial visualisation software shows certain constraints and therefore does not fully allow presenting such a wireframe model. One of the limitations is that surfaces can be displayed only if they are composed of 3 or at maximum of 4 points. Since the surfaces of buildings are generally made of more than 4 points, it is required to cut the surfaces into subsurfaces (e.g. triangles). To this end in a first step the border polygons of single building surfaces are determined. Afterwards it is tested if the polygons are "simple polygons" what means that "non adjacent edges" do not contain common points. For all "non simple polygons" a reduction to simple polygons is mandatory, e.g. after Sunday's method (Sunday 2005).

The polygons then have to be cut into triangles, what in our case is performed by a Constrained Delaunay Triangulation. It must be pointed out that a bordering polygon of a roof surface may contain another polygon of the same surface completely. This e.g. happens in case of garrets which appear within a roof surface. The central polygon then has to be excluded from the triangulation. An example for an automatically generated building model is shown in Figure 2.



Figure 2: Automatically generated building model

4 CLASSIFICATION OF DAMAGED BUILDINGS

Classification of damages in buildings affected by earthquakes presents a key research topic at Karlsruhe University since a decade (Steinle & Bähr 1999). The solutions all have to be based on comparing pre- and post event structures of the buildings under investigation. In a first step appropriate models for describing damages from the laser scanning data have to be set up.

Damaged buildings may show very different damage types. The types to be discriminated are summarised in a damage catalogue as shown in Figure 3. In detail, for each damage type descriptions and geometrical characteristics are assigned. As geometry is concerned, features are e.g. differences in height and volume as well as changes of the inclinations of the building's surfaces (Schweier & Markus 2004).

Therefore, modelling damaged buildings has to take into account such geometrical features which characterise the respective damage types well. The sequence of the approach is given in Figure 4. In a first step planar surfaces are segmented (see par. 2.2) in order to answer questions about change of inclinations and about size of the registered surfaces. In case of strong damages the segmentation results in many small surface elements and many non-segmented pixels. If a reference model of the undamaged building structure is available, an estimation is possible, whether damage occurred or not. This may be done by comparing number and size of the surfaces under concern. If no reference model is available, speculation must be done most carefully (e.g. many small surfaces might represent a dome).

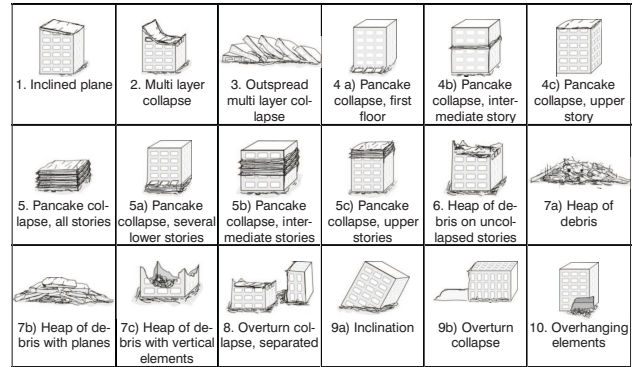


Figure 3: Compilation of the damage types (Schweier & Markus 2004)

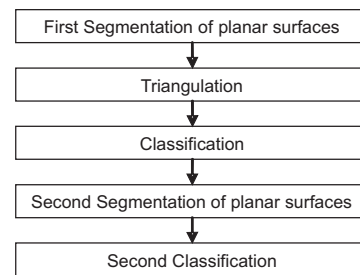


Figure 4: Workflow of the modelling of damaged buildings

After the surface segmentation a planar Delaunay-based TIN in 2.5D is produced. For the definition of the mesh points the results from the surface segmentation have to be taken into account. Therefore, points have to be selected which guarantee that the produced triangles match the adjusted planes sufficiently in segmented areas. This is the case if, for any segmented pixel, a grid point is produced with position coordinates x_P and y_P equal to the pixel coordinates and with height z_P computed in such a way that the point exactly matches the extracted plane. This height may be derived from the general equation of a plane:

$$z_P = (d - a x_P - b y_P)/c \quad (11)$$

As the non segmented points of course have to be integrated into the triangulation, too, for each pixel which was not assigned to a surface segment a point is added to the number of the mesh points, whereas its coordinates are taken from the respective pixel. For reducing the number of the created triangles, only the non segmented points and the border points of the surface segments are accepted as mesh points. Figure 5 shows the TIN of an area with damaged buildings.

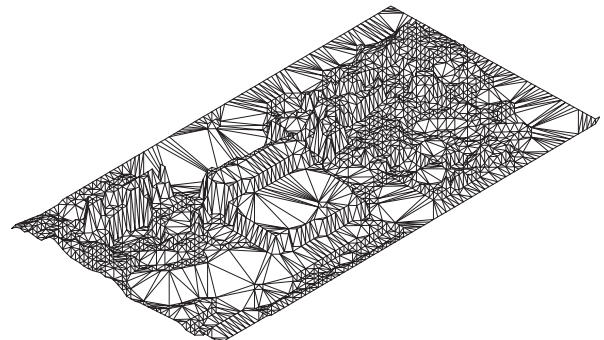


Figure 5: Produced TIN of an area with damaged buildings

Because of the ambiguity of the 2D Delaunay Triangulation in a raster domain, the TIN produced this way is not fully clear as it may lead to different results in case of regular distribution of the grid points. A 3D approach would improve this situation.

After creating the TIN the triangles have to be classified according to Figure 4. For each triangle it is tested, whether its corners were assigned by the surface segmentation process to the same segment i.e. whether the triangle is located in the associated plane. If this is true, the triangle represents a part of the assigned plane and is added to the class of *plane triangles*. It may happen that the corners of a triangle are not part of a single plane. For this type of triangle the term *planes connecting triangle* is used because it is representing a connection between two or three planar surfaces. If a triangle contains just one point which was not segmented it is classified as *debris triangle*. For such triangles the probability exists that they represent strongly damaged building parts.

Narrow shaped planar surfaces are not registered, because in the surface segmentation process a new surface segment may be created only if a seed region is found which shows a minimum area (e.g. 3 x 3 pixels) and fulfils a certain precondition (see par. 2.2). Therefore it may happen e.g. that side roofs or parts of ton-shaped roofs are represented by *debris triangles* (see par. 5).

To avoid this problem, a second segmentation is executed starting from the *debris triangles* (Figure 4). In this process it is looked for several neighbouring *debris triangles* lying approximately in a plane. The used approach is similar to the first segmentation based on raster data (see par. 2.2). The starting point is built by a *debris triangle*. First of all the parameters of the plane defined by the three points of this triangle are calculated. Afterwards it is tested for any of the neighbouring triangles if it concerns a *debris triangle*. If this is the case a regression plane is calculated through the points of the initial triangle and the points of the currently examined triangle. In order to check the correctness of the used model a global test (eq. (10)) and a test for blunders (eq. (5) and (6)) are carried out. Is the model accepted by both tests the triangles are lying approximately in a plane. So the examined triangle is assigned to the new segment. Is the assumption rejected the triangle is not assigned to the new segment and the plane parameters are reset. In both cases the next adjacent triangle is looked at. In the further steps the regression plane is calculated through the points of all triangles that have already been assigned to the new segment and the point of the momentarily considered triangle that does not belong to one of the other triangles. If no further adjacent triangle can be found that fulfils the requirements it is tested how many triangles have been assigned to the segment. If the number is less than a given number the area of the segment is regarded as too small and therefore the segment is deleted.

After the second segmentation, the triangles of course have to be classified once more. Now, two new classes are introduced: *segment triangles* and *segment/planes connecting triangles*. The first mentioned class represents newly detected surface segments. The second class contains triangles which connect new detected segments or new and old ones.

5 RESULTS

It has to be highlighted that the classification approach for damaged buildings was tested by real laser scanning data in an area of physically damaged buildings (i.e. no simulation!). The test area is a training field from the Swiss Military Disaster Relief (Figure 6). It has an extension of about 500 m x 800 m and is used for training rescue and support during catastrophic events. The



Figure 6: Aerial photograph of the test area

original data were acquired by TopoSys Company in 2004 and transformed into digital surface models of 1 m raster width. The precision of these models is in the order of ± 0.5 m in position and ± 0.15 m in height.

Figure 7 displays how a side roof of a building and a ton-shaped roof (a) look before (b) and after (c) the second surface segmentation step. The *debris triangles* are shown in red, the *planes connecting triangles* in dark and the *segment/planes connecting triangles* in light grey. Each of the extracted segments is displayed in a different colour. It is obvious, that by the first step neither the side roof nor parts of the ton-shaped roof were segmented correctly. Consequently, they are shown as debris in Figure 7 (b). After the second segmentation step the corresponding surfaces are assigned to the new surface segments.

Figure 8 shows the model of a larger area, where each surface segment is displayed by a different colour. The area contains both the building from Figure 7 of pancake collapse type and some heaps of debris. Besides, two trucks are imaged and marked by black circles. The discrimination between debris on the one hand and obsolete information like the trucks ("perturbations") on the other hand plays an important role in classification of damage types. Elements like the trucks, taken as building components, do inevitably lead to misclassifications. The example in Figure 8 clarifies, that the trucks may not be discriminated from the further debris structures without introducing additional knowledge.

A CAD model for the area shown in Figure 6 is given in Figure 9. This example shows that, supported by such a model, estimations at high probability are feasible for areas where strong damages exist and for areas where the buildings will probably not show major damages.

6 CONCLUSIONS

Modelling undamaged buildings by laser scanning is nearly operational (Kartinen et al. 2005), whereas segmentation and classification of damaged buildings is a new challenging task. Laser scanning obviously is an ideal tool for developing fast automatic real-time procedures, e.g. in the context of rescue in a disaster environment. First results are presented which use extended clas-



(a)

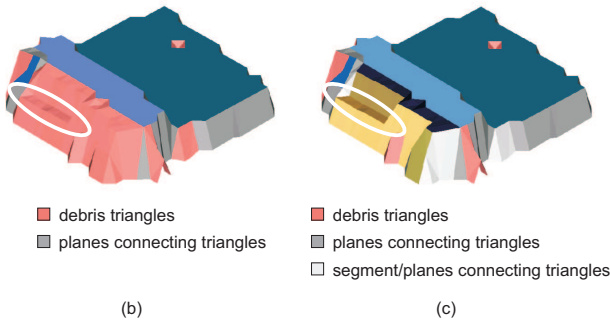


Figure 7: (a) A building with a side roof and a ton-shaped roof in a classified TIN (b) before and (c) after the second segmentation step. Each of the extracted segments is displayed in a different colour.

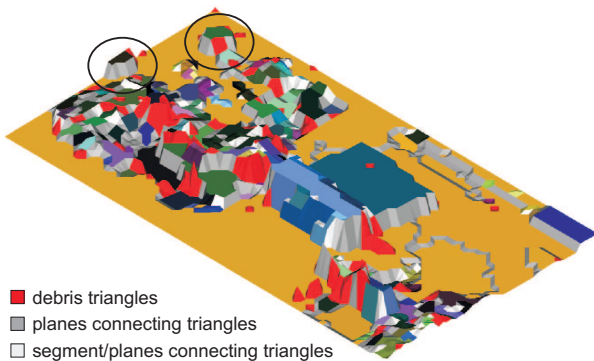


Figure 8: Model containing damaged buildings and "perturbations" (trucks marked by black circles). Each segment is shown by another colour.

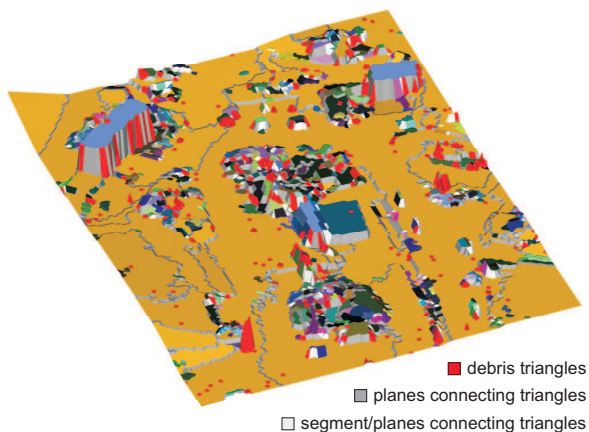


Figure 9: Model of the test area containing damaged buildings. The segments are shown in different colours.

sical approaches known from modelling of undamaged buildings and which make clear that damaged parts may be discriminated from undamaged parts of buildings.

The results are encouraging to further extend the approach: As far as the algorithms are concerned, much more should be possible to extract from the TIN than just geometrical parameters, especially when modelling in 3D instead of 2D. For instance, neighbourhood and shape are important additional features to take into consideration. Besides refinement of the algorithms additional data is expected to strongly improve the results. The step to fuse multispectral scanner and laser scanning data suggests itself as today the flights do provide both.

ACKNOWLEDGEMENTS

The authors would like to thank the German Research Foundation, Collaborative Research Centre 461 (DFG SFB 461) for financial support and the Swiss Disaster Relief Coordination and Control Center DDPS for providing their facilities.

REFERENCES

Baarda, W., 1967. Statistical concepts in geodesy. Publications on geodesy 2(4), Netherlands Geodetic Commission.

Baarda, W., 1968. A testing procedure for use in geodetic networks. Publications on geodesy 2(5), Netherlands Geodetic Commission.

Bähr, H.-P. and Müller, M., 2004. Graphics and Language as Complementary Formal Representations for Geospatial Descriptions. International Archives of Photogrammetry, Remote Sensing and Spatial Information Sciences XXXV, Part B, Comm. 4, Istanbul, Turkey, pp. 216-221.

Bähr, H.-P., 2005. Sprache - ein Datentyp der Bildanalyse. In: H.-P. Bähr and T. Vögtle (eds), *Digitale Bildverarbeitung - Anwendungen in Photogrammetrie, Fernerkundung und GIS*, Wichmann Verlag, Heidelberg, 4. edn., pp. 211-228.

Bronstein, I. N., Semendjajew, K. A., Musiol, G. and Mühlig, H., 2001. Taschenbuch der Mathematik. Unchanged reprint of the 5. edn., Verlag Harri Deutsch, Thun and Frankfurt/Main.

Heck, B., 1985. Ein- und zweidimensionale Ausreißertests bei der ebenen Helmert-Transformation. *Zeitschrift für Vermessungswesen* 110(10), pp. 461-471.

Kaartinen, H., Hyypää, J., Gülch, E., Vosselman, G., Hyypää, H., Matikainen, L., Hofmann, A.D., Mäder, U., Persson, Å., Söderman, U., Elmqvist, M., Ruiz, A., Dragoja, M., Flamanc, D., Maillet, G., Kersten, T., Carl, J., Hau, R., Wild, E., Frederiksen, L., Holmgaard, J. and Vester, K., 2005. Accuracy of 3D city models: EuroSDR comparison. International Archives of Photogrammetry, Remote Sensing and Spatial Information Sciences XXXVI, Part 3/W19, Enschede, The Netherlands, pp. 227-232.

Niemeier, W., 2002. *Ausgleichsrechnung*. Walter de Gruyter, Berlin.

Schwalbe, E., Maas, H.-G., Seidel, F., 2005. 3D building model generation from airborne laserscanner data using 2D GIS data and orthogonal point cloud projections. International Archives of Photogrammetry, Remote Sensing and Spatial Information Sciences XXXVI, Part 3/W19, Enschede, The Netherlands, pp. 209-214.

Schweier C. and Markus M., 2004. Assessment of the search and rescue demand for individual buildings. In: Proceedings of the 13th World Conference on Earthquake Engineering, Vancouver, Canada.

Steinle E. and Bähr H.-P., 1999. Laserscanning for change detection in urban environment. In: O. Altan and L. Gründig (eds), *Proceedings of the Third Turkish-German Joint Geodetic Days - Towards A Digital Age*, Volume I, Istanbul, Turkey, pp. 147-156.

Steinle, E., 2005. Gebäudemodellierung und -änderungserkennung aus multitemporalen Laserscanningdaten. PhD dissertation, Deutsche Geodätische Kommission, Reihe C, Heft Nr. 594, Verlag der Bayerischen Akademie der Wissenschaften, München, http://129.187.165.2/typo3_dgk/docs/c-594.pdf (accessed 28 Feb. 2006).

Sunday, D., 2005. Intersections for a 2D Set of Segments. http://www.geometryalgorithms.com/Archive/algorithm_0108/algorithm_0108.htm (accessed 19 Dec. 2005).

Vögtle, T. and Steinle, E., 2000. 3D Modelling of Buildings Using Laser Scanning and Spectral Information. International Archives of Photogrammetry and Remote Sensing XXXIII, Part B3, Amsterdam, The Netherlands, pp. 927-934.